Journal of Molecular Catalysis A: Chemical 320 (2010) 14–18

Contents lists available at ScienceDirect

Journal of Molecular Catalysis A: Chemical

journal homepage: www.elsevier.com/locate/molcata

Gas phase photocatalytic oxidation of toluene using highly active Pt doped TiO_2

G. Colón[a,*], M. Maicu[a], M.C. Hidalgo[a], J.A. Navío[a], A. Kubacka[b], M. Fernández-García[b]

[a] Instituto de Ciencia de Materiales de Sevilla, Centro Mixto Universidad de Sevilla-CSIC, C/Américo Vespucio s/n, 41092 Sevilla, Spain
[b] Instituto de Catálisis y Petroleoquímica, CSIC, C/Marie Curie 2, 28049 Madrid, Spain

ARTICLE INFO

Article history:
Received 5 October 2009
Received in revised form
16 December 2009
Accepted 18 December 2009
Available online 4 January 2010

Keywords:
Platinum
Sulphated TiO_2 photocatalyst
Titania
Anatase
Defects
XPS
Toluene

ABSTRACT

Platinum doped TiO_2 materials were studied for the gas phase photocatalytic degradation of toluene. Platinum deposition was achieved by photodeposition method over TiO_2 prepared by means of a sol–gel route. The effect of sulphuric acid pretreatment on the further platinisation process has been extensively studied. From the wide structural and surface analysis of the catalysts an interesting synergetic effect has been demonstrated. The previous sulphate treatment over TiO_2 leads to improved dispersion of the Pt which presents a lower aggregation and homogeneous cluster size. This fact, together with the adequate control of anatase structural and surface parameter due to the sulphate treatment, renders a good photocatalytic performance for toluene oxidation reaction. The highest reaction rates and CO_2 selectivities have been obtained for Pt–S–TiO_2 samples.

1. Introduction

The improvement and optimisation of TiO_2 as a photocatalyst is an important task for technical applications of heterogeneous photocatalysis in the future. In this sense, many investigations on the basic principles and enhancement of the photocatalytic activity either in the ultraviolet or visible have been carried out [1,2]. The activity of a TiO_2 powder depends on its bulk and surface properties. Moreover, the improvement of the final photocatalytic properties might be achieved by influencing those properties which control either the charge carrier dynamics (carrier generation, transfer and diffusion) or the surface catalytic process, which are the quality of the structure and the surface features. Thus, different options have been investigated and widely reported in the literature, such as surface sensitization [3,4], control of structure and particle size of the titania [5], cationic and anionic doping [6,7] or surface modification with noble metals [8,9]. Among noble metals, platinum has been one of the most used metals for TiO_2 surface modification [10]. The particular case of platinisation has been controversial and the reported experimental results appear contradictory with respect to the effect on the final photocatalytic activity [10–12]. Therefore, the degree of the TiO_2 photoactivity enhancement by platinisation seems to be highly dependent on several factors such as the substrate to be degraded [11,13], the properties and amount of platinum deposited [8] and structural and morphological properties of original TiO_2 [14,15].

It is assumed that some of the photogenerated electrons would interact with platinum states and be spatially separated from holes leading to a better separation of charge carriers [16]. Therefore, the surface situation of Pt deposits would strongly influence the electronical mechanism of the photocatalytic reaction.

In previous papers, we have stated that the deposition of noble metal over sulphate pretreated TiO_2 significantly affect to its size and dispersion [8,9]. Thus, the enhancement factors observed for the phenol photocatalytic degradation on Pt and Au doped TiO_2 appear notably higher for presulphated systems. In the present paper we study the evolution of toluene gas phase photocatalytic degradation over Pt–TiO_2 systems.

2. Experimental

As previously reported [17], TiO_2 was prepared by a sol–gel method using titanium tetraisopropoxide (TTIP) as precursor in isopropanol (3.9 ml TTIP in 200 ml iPrOH). Hydrolysis of the isopropanol-TTIP solution was achieved by adding certain volume of bidistilled water (TTIP:H_2O = 0.05). The precipitate was then filtered and dried at 120 °C overnight and divided in two portions. Sulphation of one of the batch was performed by dispersing the fresh dried powders in a H_2SO_4 1 M solution (50 ml g^{-1}) for 1 h. Then, the suspension was filtered off and the powder dried again

* Corresponding author. Tel.: +34 954489536; fax: +34 954460665.
E-mail address: gcolon@icmse.csic.es (G. Colón).

1381-1169/$ – see front matter © 2010 Elsevier B.V. All rights reserved.
doi:10.1016/j.molcata.2009.12.009

Table 1
Surface and structural characterization results.

Catalyst	S_{BET} (m^2/g)	Average pore diameter, D_p (Å)	Crystallite size (nm)	Pt content XRF (wt%)
TiO_2	40.6	~45	17	–
Pt–TiO_2 1.5%	39.1	~45	19	1.40
Pt–TiO_2 2.5%	43.0	~45	18	2.82
S–TiO_2	19.1	~135	31	–
Pt–S–TiO_2 1.5%	19.1	~135	31	1.49
Pt–S–TiO_2 2.5%	20.6	~135	29	2.63

at 120 °C overnight. For non-sulphated TiO_2, the dried precipitate was just calcined at 500 °C for 2 h. For sulphated TiO_2, the dried precipitate was impregnated by a sulphuric acid 1 M solution for 1 h, then filtered again, dried at 110 °C overnight and calcined at 700 °C for 2 h, following the same procedure of our previous work. These calcination temperatures were chosen in order to compare best samples in both series regarding photocatalytic activity for phenol degradation, i.e., 500 °C for non-sulphated TiO_2 and 700 °C for sulphated TiO_2 [17].

Platinisation was performed over the calcined TiO_2 samples by photodeposition of platinum from hexachloroplatinic (IV) acid (H_2PtCl_6, Merck 40% Pt) following a modification of a method described elsewhere [8]. Suspensions of the different TiO_2 in distilled water were prepared (5 g TiO_2 L^{-1}) adding isopropanol to act as sacrificial agent (0.3 M final concentration) and the appropriate amount of H_2PtCl_6 for different nominal amounts of deposited Pt (1.5 and 2.5 wt% total to TiO_2) under continuous nitrogen sparging. Photodepositions were performed by illumination of the suspensions for 6 h with a medium pressure mercury lamp (400 W) of photon flux ca. 2.6×10^{-7} einstein s^{-1} L^{-1} in the region of wavelengths <400 nm. After recovering of the powders by filtration, samples were dried at 110 °C overnight. To assure reproducibility of the preparation method, selected samples were independently prepared twice, and the reproducibility in structural and morphological as well as in activity results was confirmed.

BET surface area and porosity measurements were carried out by N_2 adsorption at 77 K using a Micromeritics 2010 instrument.

X-ray diffraction (XRD) patterns were obtained using a Siemens D-501 diffractometer with Ni filter and graphite monochromator. The X-ray source was Cu Kα radiation. The line broadening of X-ray diffraction peak corresponding to anatase phase planes was determined by deconvolution of the corresponding peak using a Voigt function. Crystallite sizes of the different phases were estimated from the line broadening of the corresponding X-ray diffraction peaks by using the Scherrer equation.

The morphology of samples was followed by means of Field Emission SEM (Hitachi S 4800). The samples were dispersed in ethanol using an ultrasonicator and dropped on a copper grid.

UV–vis spectra were recorded in the diffuse reflectance mode (R) and transformed to a magnitude proportional to the extinction coefficient (K) through the Kubelka–Munk function, $F(R_\infty)$. Samples were mixed with $BaSO_4$ that does not absorb in the UV–vis radiation range (white standard). Scans range was 240–800 nm.

XPS data were recorded on 4×4 mm^2 pellets, 0.5 mm thick, prepared by slightly pressing the powdered materials which were outgassed in the prechamber of the instrument at 150 °C up to a pressure $<2 \times 10^{-8}$ Torr to remove chemisorbed water from their surfaces. The Leybold-Heraeus LHS10 spectrometer main chamber, working at a pressure $<2 \times 10^{-9}$ Torr, was equipped with an EA-200 MCD hemispherical electron analyzer with a dual X-ray source working with Al Kα ($h\nu$ = 1486.6 eV) at 120 W, 30 mA using C *1s* as energy reference (284.6 eV). Surface chemical compositions were estimated from XP-spectra, by calculating the integral of each peak after subtraction of the *"S-shaped"* Shirley-type background using the appropriate experimental sensitivity factors [18].

Activity and selectivity for the gas-phase photooxidation of toluene were tested in a continuous flow annular photoreactor [19]. The corresponding amount of catalyst was suspended in 1 ml of water, painted on a Pyrex tube (cut off at ca. 290 nm) and dried at room temperature. Thus, ca. 30 mg of photocatalyst is disposed as a thin layer coating on the Pyrex tube showing an irregular thickness of ca. 40 μm. In any case, the reaction rates measured and reported were independent of the film thickness in the 20–60 μm range. The reacting mixture (100 ml min^{-1}) was prepared by injecting toluene (Panreac, spectroscopic grade) into a wet (ca. 75% relative humidity, RH) 20 vol.% O_2/N_2 flow before entering at room temperature to the photoreactor, yielding an organic inlet concentration of ca. 800 ppmv. Under such conditions, the reaction rate shows a zero order kinetic following a Langmuir–Hinshelwood mechanism with respect to the total flow and hydrocarbon/oxygen concentrations. After flowing the mixture for 1 h (control test) in the dark, the catalyst was irradiated by four fluorescent daylight lamps (6 W, Sylvania F6W/D) with a radiation spectrum simulating sunlight (UV content of 3%), symmetrically positioned outside the photoreactor. Reference experiments with UV lamps (Sylvania F6WBLT-65; 6 W, max. at ca. 350 nm) were run using the same reaction set-up and procedure. Reaction rates were evaluated (vide supra) under steady state conditions, typically achieved after 3–4 h from the irradiation starting. No change in activity was detected for all samples within the next 6 h. The concentration of reactants and products was analyzed using an on-line gas chromatograph (Agilent GC 6890) equipped with HP-PLOT-Q/HP-Innowax columns (0.25 mm I.D. × 30 m) and TCD/FID detectors.

3. Results and discussions

BET surface area values for the samples are shown in Table 1. As it can be seen, the non-sulphated series presented BET surface area values around 39 m^2/g while sulphated samples presented values around 20 m^2/g. The smaller surface area of the sulphate series can be ascribed to the higher calcination temperature used in the preparation of these samples, though a notably stabilization is achieved due to sulphate pretreatment. It can be also noticed that the BET surface area values were not affected by the platinisation process.

Crystalline phase compositions of all samples were studied by XRD and results are presented in Fig. 1. As it can be noticed from XRD patterns, the non-sulphated series as well as the sulphated one, showed only anatase phase. Indeed, it has been previously shown that sulphuric acid pre-treatment of TiO_2 stabilizes anatase phase against sintering and phase transformation into rutile up to calcination temperature as high as 700 °C. This stabilization of anatase phase as well as of surface area (Table 1) could be explained by taking into account the presence of sulphate groups anchored on the TiO_2 precursor before calcination. During calcinations, the surface sulphate groups are removed and subsequently, reaching temperatures higher than 650 °C a fast rutilisation process takes place [17,20]. Furthermore, a vacancy creation process is driven by a dehydroxylation process of the excess of adsorbed protons during calcination and leads to the generation of a highly defective material with stabilized defects at near surface regions [20].

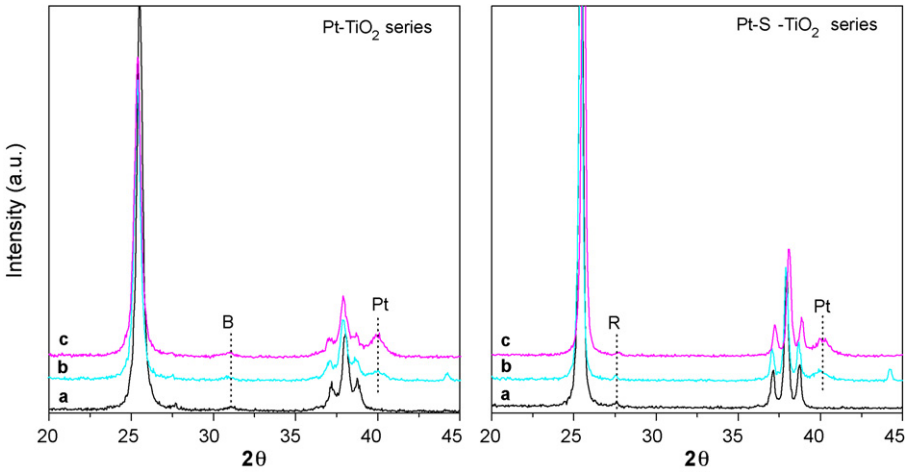

Fig. 1. XRD patterns corresponding to Pt–TiO_2 and Pt–S–TiO_2 series: (a) unplatinised, (b) 1.5% Pt and (c) 2.5% Pt.

The subsequent platinisation process does not modify the surface area or phase composition. For platinised samples it is detectable the diffraction peaks corresponding to Pt denoting the presence of the metal cluster after the photodeposition process. The anatase crystalline domains for the samples, estimated by the Scherrer equation, are presented in Table 1.

The analysis of metal size and dispersion has been studied by TEM (not shown). Photodeposited platinum-clusters were spherical shape, presenting a higher dispersion for sulphated samples at low metal loading. An estimation of the main average platinum particle size of the samples was made by counting platinum particles in a high number of TEM micrographs (Fig. 2). The photodeposition of platinum produces small metal clusters of around 2–5 nm. Moreover, for samples with 1.5% of Pt, it can be inferred that samples with sulphated pretreatment presented smaller platinum deposits, denoting that the photodeposition method is influenced by the previous sulphation.

From the UV–vis spectra we have calculated the band gap values for the studied samples (Fig. 3). Sulphated and non-sulphated series presented similar band-gap values, around 3.2–3.3 eV in any case. The small differences observed are within the experimental error (±0.1 eV). Comparison between the diffuse reflectance spectra of platinised and non-platinised samples showed no differences in the UV range. However, platinised samples show a stronger absorption respect to unmodified samples throughout the visible range. Thus, it is possible to identify absorptions located at 465, 530 and 710 nm associated to the presence of Pt.

Total platinum content in the samples was determined by XRF (values shown in Table 1). From these values, it is inferred that the bulk contents of platinum are in all cases close the theoretical nominal loadings. Consequently, the platinisation process by the described photodeposition method leads to a reasonable coating yield. Regarding to the surface analysis performed by XPS, for samples with the same nominal platinum loading, surface data showed a higher content of the metal for sulphated samples (Table 2). Even taking into account the different BET surface area between both series (Table 1), sulphated samples showed a higher surface amount of platinum than non-sulphated ones. XPS is a surface sensitive

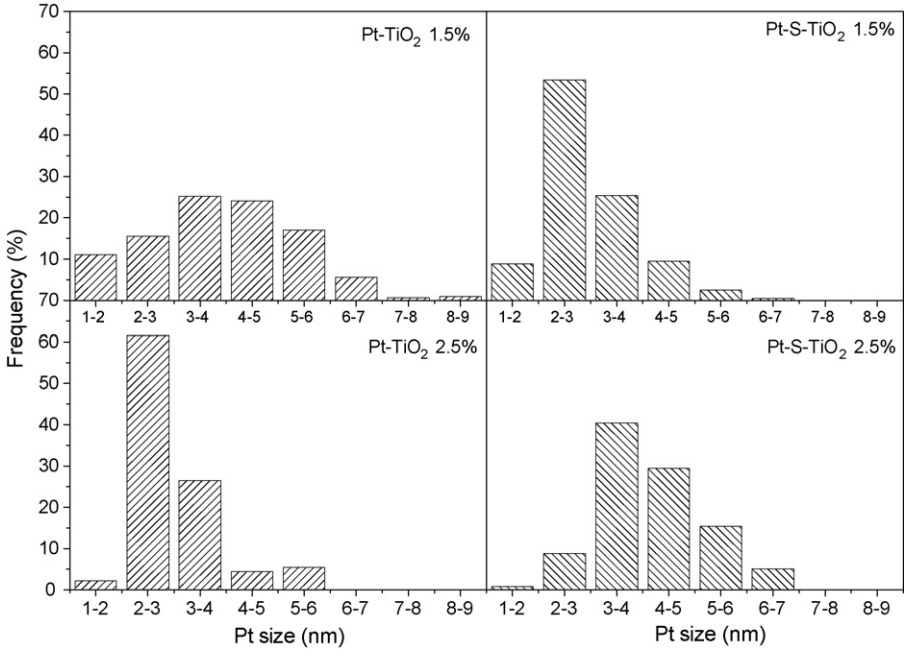

Fig. 2. Platinum size distribution calculated from TEM images.

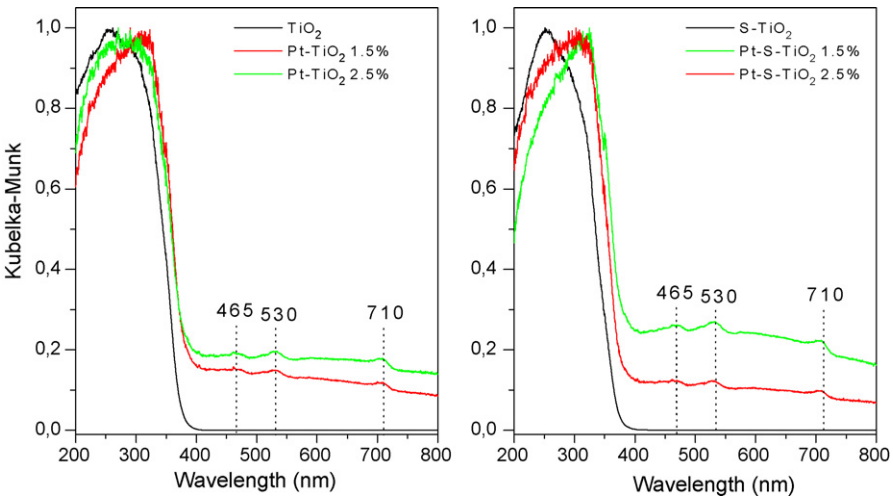

Fig. 3. Uv–vis diffuse reflectance spectra for Pt–TiO_2 and Pt–S–TiO_2 series.

technique which gives information about platinum dispersion over the TiO_2. For samples with the same total amount of platinum, the sample with a higher dispersion of the metal on the surface might show a higher signal peak for platinum in the XPS spectrum because of the high coverage of TiO_2 surface [21]. Therefore, and in agreement with TEM observations, sulphate pre-treatment of TiO_2 leads to a higher metal dispersion on the TiO_2 surface [8,9].

The platinum oxidation state is reported to have a strong influence in the photocatalytic properties of Pt-doped TiO_2 systems. Thus, it is generally accepted that Pt^0 is the most favourable oxidation state for photocatalytic reaction [22]. In Fig. 4 we present the Pt *4f* region for selected pairs of samples. The main XPS doublet located ca. 70.2 and 73.6 eV would correspond to metallic Pt. In addition, other two less prominent contributions can be resolved with $4f_{7/2}$ signals located at ca. 71.5 and 73.1 eV. These other doublets would be associated to Pt^{2+} and Pt^{4+}, respectively [23,24]. Thus, a small amount of Pt^{2+} and Pt^{4+} species is present in Pt photodeposited clusters.

Regarding to the O/Ti ratio, in S–TiO_2 sample this value is clearly bellow the stoichiometric one. This fact was already described by us and was associated to the sulphate pretreatment submitted in this sample. Therefore, it can be assumed that a certain number of oxygen vacancies might be present at the near surface region. After platinisation, sulphated samples seem to recover the stoichiometric situation. The loss of the oxygen vacancies during the platinisation process would indicate their annihilation while platinum is reduced.

The steady rate and selectivity values obtained Pt-containing samples in the toluene gas-phase photocatalytic oxidation are shown in Fig. 5. Only CO_2 and benzaldehyde were detected during reaction as gaseous products. For comparison, the photocatalytic parameters obtained for commercial Degussa P25 are also included in this figure.

Table 2
Surface analysis results from XPS.

Catalyst	Binding energy (eV) Pt $4f_{7/2}$	Pt (% at)	Pt (wt%)	O/Ti
TiO_2	–	–	–	1.90
Pt–TiO_2 1.5%	70.2	0.33	2.36	1.92
Pt–TiO_2 2.5%	70.2	0.42	3.05	1.96
S–TiO_2	–	–	–	1.70
Pt–S–TiO_2 1.5%	70.3	0.82	6.02	1.95
Pt–S–TiO_2 2.5%	70.3	0.63	4.65	1.99

From the reactivity results showed in Fig. 5, it is firstly inferred an enhanced toluene photooxidation steady rate on doping the titania structure with platinum. The initial slight improvement observed for sulphate pretreated TiO_2 with respect to untreated one is notably enhanced when Pt is supported at the TiO_2 surface. Thus, the enhancement factors (Ef) calculated from the reaction

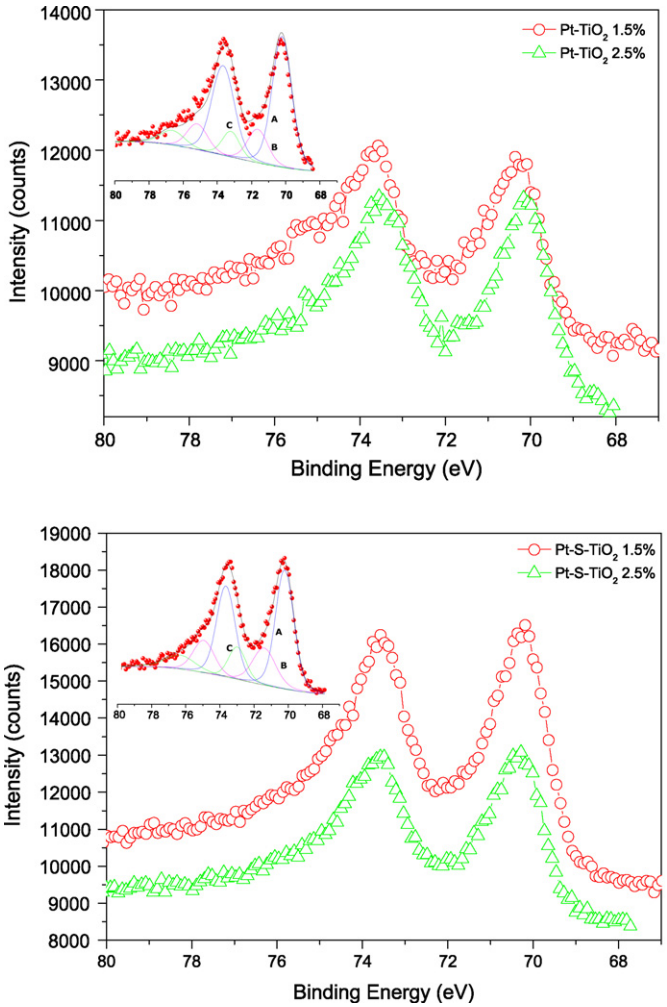

Fig. 4. XPS spectra in the Pt *4f* region for Pt–TiO_2 and Pt–S–TiO_2 series.

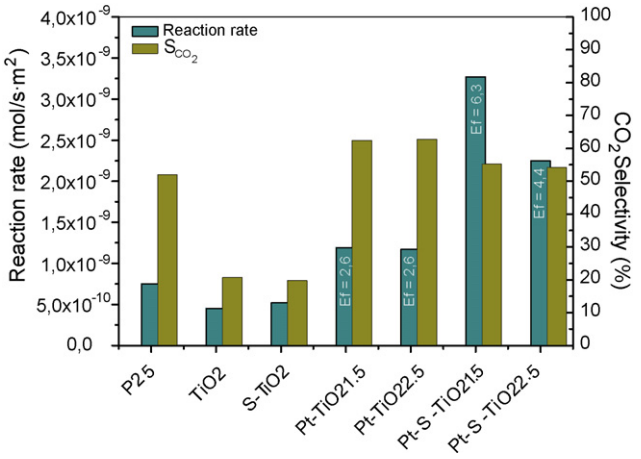

Fig. 5. Reaction rates and CO_2 selectivity for toluene degradation reaction.

rates clearly denote the synergetic effect occurring by the deposition of Pt over presulphated TiO_2. The maximum value, e.g. 6.3, is among the largest reported so far [10]. The Ef values also show that while for unsulphated TiO_2 the amount of Pt do not induce an associated increase in the photoactivity, for S–TiO_2 series a maximum in the Pt loading seem to be present. Consequently, platinum doped S–TiO_2 samples show the best photoactivity for 1.5 wt% loading of Pt. This result is in accordance to previous evolution of these systems for the phenol photocatalytic degradation in liquid phase. If we consider the evolution of Pt surface concentration measured by XPS vs. the obtained from XRF, it is clear that for non-sulphated TiO_2 a higher nominal Pt content leads to a higher surface content. On the contrary, for sulphated series after 1.5% Pt the surface content observed from XPS seems to decrease. This would mean that for sulphated TiO_2 an aggregation is occurring for loadings higher than 1.5% (Fig. 2). In the case of non-sulphated TiO_2 the Pt clusters sizes are slightly larger, indicating that the aggregation of the noble metal phase is taking place already at this lower Pt concentration [8].

Under the experimental conditions of this study, during toluene photo-oxidation the only reaction products observed are CO_2 and benzaldehyde. Upon a humidified flow, the catalyst surface is expected to be partially covered with water and have less toluene adsorbed. At high humidity level (as is here the case) partial oxidation products are likely favoured, and thus the complete mineralization is not likely achieved. Moreover, Anpo et al. [25] have claimed that the presence of water in the toluene photocatalytic oxidation reaction enhances the efficiency of electron–hole recombination. On the counterpart, the presence of water allows stable operation over prolonged time periods and limits the formation of undesired, noxious reaction products [26,27]. In this sense, it has been reported that more adsorbed water may increase the capacity of the catalyst for the removal of the adsorbed intermediates that causes deactivation [28]. Thus, the addition of water appears to increase both the rate of toluene oxidation to strongly bound intermediates and the oxidation rate of such intermediates to CO_2 [29].

The CO_2 selectivity showed by unplatinised TiO_2 (sulphated and unsulphated) is similar and quite lower than that exhibited by P25. On the contrary, values displayed by Pt doped TiO_2 systems significantly increase in the selectivity to CO_2 and therefore the toluene mineralization. This fact differs from those already described for Pt–W doped TiO_2 [30]. In this sense, authors reported a high benzaldehyde selectivity showed by the platinised systems by considering a hampering to benzaldehyde photooxidation when Pt is present. However, the nature and oxidation state of Pt species in that case was presumably different since the deposition was achieved by incipient wetness. The increment in CO_2 selectivity was also accompanied by a drastic growth in the photocatalytic oxidation reaction rate for the S–TiO_2 systems.

4. Conclusions

A synergetic affect between platinisation and sulphate pretreatment of TiO_2 was found for the photocatalytic activity of sol–gel prepared TiO_2. Samples simultaneously sulphated and platinised obtained a remarkable improvement of the toluene photocatalytic oxidation. Sulphated pre-treatment clearly stabilized the structural and surface features of the TiO_2 against sintering. Upon Pt deposition, sulphate pretreatment of TiO_2 produces a higher dispersion and smaller average deposit size of platinum. Both factors contributed to the higher photocatalytic activity of these samples compared to the non-sulphated series. The best photocatalytic activities were obtained for Pt doped and sulphate pretreated systems, showing high CO_2 selectivities and a notably higher enhancement factor. These results clearly overcome the commercial TiO_2 Degussa P25.

Acknowledgments

Financial support by Junta de Andalucía (P.A.I.D.I. group FQM-181 annual funding and Project P06-FQM-1406) and CICYT (CTQ2007-60480/BQI and CTQ2008-05961-C02-01) is acknowledged. A.K. thanks the CSIC for a I3P Postdoctoral grant.

References

[1] G. Colón, C. Belver, M. Fernández-García, in: M. Fernández-García, J.A. Rodríguez (Eds.), Synthesis, Properties and Application of Oxide Nanoparticles, Wiley, USA, 2007, ISBN 978-0-471-72405-6.
[2] O. Carp, C.L. Huisman, A. Reller, Prog. Solid State Chem. 32 (2004) 33.
[3] K. Szaciłowski, W. Macyk, A. Drzewiecka-Matuszek, M. Brindell, G. Stochel, Chem. Rev. 105 (2005) 2647.
[4] S. Gawęda, G. Stochel, K. Szaciłowski, J. Phys. Chem. C 112 (2008) 19131.
[5] M.C. Hidalgo, M. Aguilar, M. Maicu, J.A. Navío, G. Colón, Catal. Today 129 (2007) 50.
[6] A. Kubacka, M. Fernández-García, G. Colón, J. Catal. 254 (2008) 272.
[7] A. Kubacka, B. Bachiller-Baeza, G. Colón, M. Fernández-García, J. Phys. Chem. C 113 (2009) 8553.
[8] M.C. Hidalgo, M. Maicu, J.A. Navío, G. Colón, Appl. Catal. B: Environ. 81 (2008) 49.
[9] M.C. Hidalgo, M. Maicu, J.A. Navío, G. Colón, J. Phys. Chem. C 113 (2009) 12840.
[10] S.K. Lee, A. Mills, Platinum Met. Rev. 47 (2003) 61.
[11] F. Denny, J. Scott, K. Chiang, W.Y. Teoh, R. Amal, J. Mol. Catal. A 263 (2006) 93.
[12] B. Sun, A.V. Vorontsov, P.G. Smirniotis, Langmuir 19 (2003) 3151.
[13] U. Siemon, D. Bahnemann, J.J. Testa, D. Rodríguez, M.I. Litter, N. Bruno, J. Photochem. Photobiol. A 148 (2002) 247.
[14] C.A. Emilio, M.I. Litter, M. Kunst, M. Bouchard, C. Colbeau-Justin, Langmuir 22 (2006) 3606.
[15] M.C. Hidalgo, M. Maicu, J.A. Navío, G. Colón, Catal. Today 129 (2007) 43.
[16] K.M. Schindler, M. Kunst, J. Phys. Chem. 94 (1990) 8222.
[17] G. Colón, M.C. Hidalgo, J.A. Navío, Appl. Catal. B: Environ. 45 (2003) 39.
[18] D. Briggs, M.P. Seah, Practical Surface Analysis by Auger and X-Ray Photoemission Spectroscopies, John Wiley, New York, 1983.
[19] A.J. Maira, K.L. Yeung, J. Soria, J.M. Coronado, C. Belver, C.Y. Lee, V. Augugliaro, Appl. Catal. B: Environ. 29 (2001) 327.
[20] G. Colón, M.C. Hidalgo, G. Munuera, I. Ferino, M.G. Cutrufello, J.A. Navío, Appl. Catal. B: Environ. 63 (2006) 45.
[21] I. Chorkendorff, J.W. Niemantsverdriet, Concepts of Modern Catalysis and Kinetics, Wiley–VCH Verlag, Weinheim, 2003.
[22] J. Lee, W. Choi, J. Phys. Chem. B 109 (2005) 7399.
[23] Z. Jin, Z. Chen, Q. Li, C. Xi, X. Zheng, J. Photochem. Photobiol. A 81 (1994) 177.
[24] G. Wang, Y. Lin, X. Xiao, X. Li, W. Wang, Surf. Int. Sci. 36 (2004) 1437.
[25] D.R. Park, J. Zhang, K. Ikeue, H. Yamashita, M. Anpo, J. Catal. 185 (1999) 114.
[26] T. Guo, Z. Dai, C. Wu, T. Zhu, Appl. Catal. B 79 (2008) 171.
[27] M. Sleiman, P. Conchon, C. Ferronato, J.-M. Chovelon, Appl. Catal. B: Environ. 86 (2009) 159.
[28] F. Fresno, M.D. Hernández-Alonso, D. Tudela, J.M. Coronado, J. Soria, Appl. Catal. B: Environ. 84 (2008) 598.
[29] M. Catherine Blount, J.L. Falconer, Appl. Catal. B: Environ. 39 (2002) 39.
[30] M. Fernández-García, A. Fuerte, M.D. Hernández-Alonso, J. Soria, A. Martínez-Arias, J. Catal. 245 (2007) 84.